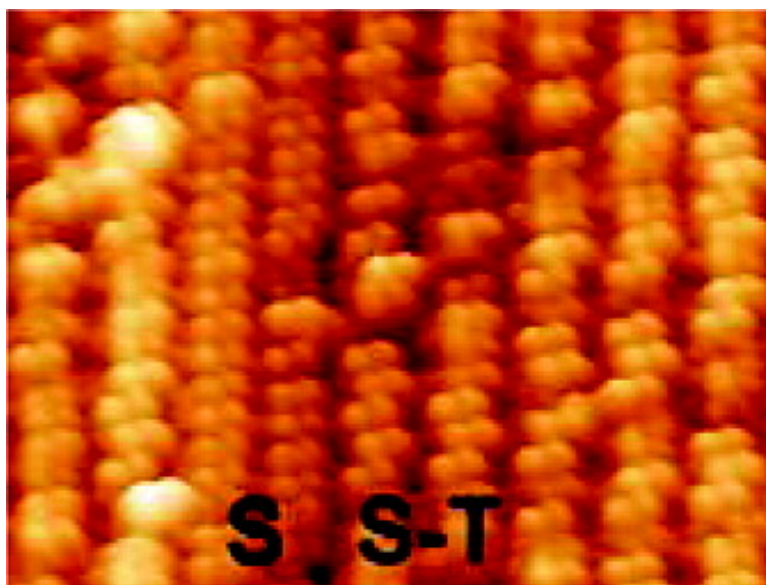


Complete Supramolecular Self-Assembled Adlayer on a Silicon Surface at Room Temperature

Younes Makoudi, Frank Palmino, Madjid Arab, Eric Duverger, and Frederic Che#rioux

J. Am. Chem. Soc., **2008**, 130 (21), 6670-6671 • DOI: 10.1021/ja8001259 • Publication Date (Web): 07 May 2008

Downloaded from <http://pubs.acs.org> on February 8, 2009



More About This Article

Additional resources and features associated with this article are available within the HTML version:

- Supporting Information
- Links to the 1 articles that cite this article, as of the time of this article download
- Access to high resolution figures
- Links to articles and content related to this article
- Copyright permission to reproduce figures and/or text from this article

[View the Full Text HTML](#)



ACS Publications
High quality. High impact.

Complete Supramolecular Self-Assembled Adlayer on a Silicon Surface at Room Temperature

Younes Makoudi, Frank Palmino, Madjid Arab, Eric Duverger, and Frédéric Chérioux*

Institut FEMTO-ST, CNRS, Université de Franche Comté, 32 Avenue de l'Observatoire, F-25044 Besançon cedex, France

Received January 7, 2008; E-mail: frederic.cherieux@femto-st.fr

The controlled positioning and assembling of polyfunctional molecules on surfaces are attracting considerable interest.¹ For example, in the view to create new electronic devices, physicists have had to rely increasingly on the originality of chemists in designing molecular systems possessing useful properties.² A rich variety of molecular nanostructures such as clusters, wires, and extended 2D networks have been selectively assembled on surfaces and directly characterized by scanning tunneling microscopy (STM). In this approach, the selective molecular assembly has been controlled by tuning directional intermolecular attractions such as hydrogen bonds or Van der Waals interactions.³ Many remarkable examples of such complex architectures have been obtained by supramolecular self-assembly on metallic⁴ or HOPG⁵ substrates. Nevertheless, the use of semiconductive interfaces remains one of the best choices for the development of operational post-CMOS devices. Despite numerous attempts, the observation of complete organic molecules adlayer on semiconductive substrates has not been reported in the literature yet. This failure could be explained by strong molecule-substrate interactions (for example the formation of Si-C σ bonds), which can disrupt the growth of the supramolecular edifice.⁶ Recently, several strategies have emerged to prevent the formation of covalent bonds with silicon surfaces: (i) passivation of the surface by inserting doping elements (for example B or C atoms)⁷ (ii) overriding of the adsorbate-substrate interactions by the formation of strong supramolecular dimers,⁸ or (iii) shielding the π -skeleton by the insertion of charged atoms.⁹ In this paper, we are detailing the engineering of a complete adlayer of organic nanolines by supramolecular self-assembly on Si(111)-B $\sqrt{3x\sqrt{3}R30^\circ}$ surface at room temperature. This breakthrough has been achieved thanks to the combination of boron atoms used as doping elements to passivate the silicon-based surface, with the formation of strong hydrogen bonds between pairs of dipolar molecules.

To circumvent the problem of silicon surface reactivity with π -conjugated molecules, the Si(111)-B $\sqrt{3x\sqrt{3}R30^\circ}$ surface has been used as substrate. This surface possesses the unique particularity to show depopulated dangling bonds due to the presence of boron atoms underneath the top silicon layer, leading to a weak interaction π -conjugated organic molecules/surface.^{7b} Therefore, the growth of the supramolecular edifice should be only controlled by the molecule-molecule interactions as reported in most work using metallic substrates.

All STM experiments were performed with an Omicron microscope and were carried out in an ultrahigh vacuum chamber with a pressure lower than 2×10^{-10} mbar. STM images were acquired in constant-current mode at room temperature. 4-Aminobenzonitrile were purchased from Aldrich and purified by column chromatography (silica gel, petroleum ether as eluent) and then, by recrystallization (ethanol) before being used. 4-Aminobenzonitrile are push-pull molecules where the amino function is the donor group and CN is the electron withdrawing group. The length of the

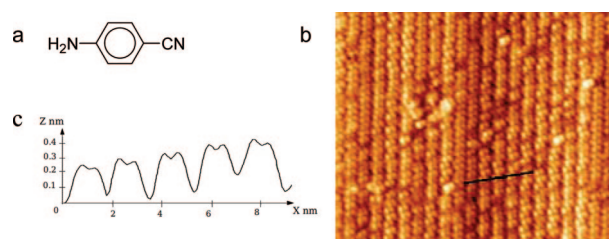


Figure 1. (a) Chemical structure of 4-aminobenzonitrile; (b) large scale STM image of the nanolines network constituted by the adsorption 4-aminobenzonitrile on Si(111)-B $\sqrt{3x\sqrt{3}R30^\circ}$ surface at room temperature ($40 \times 32 \text{ nm}^2$, $V_s = -1.7 \text{ V}$, and $I = 0.6 \text{ nA}$); (c) z-profile along the dark line.

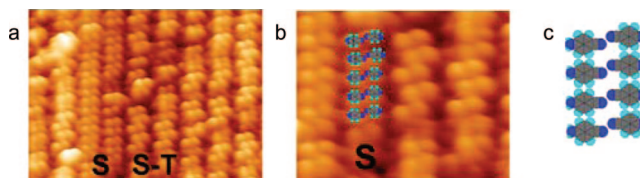


Figure 2. (a) High-resolution STM image ($16 \times 15 \text{ nm}^2$) of the two types of nanolines of the 4-aminobenzonitrile adlayer with (S) straight nanowire and (S-T) saw-toothed nanowire; (b) superimposed ball model of 4-aminobenzonitrile on straight nanolines on an STM image ($7.5 \times 8.8 \text{ nm}^2$) and (c) ball model of 4-aminobenzonitrile in antiferroelectric conformation. The imaging conditions were $V_s = -1.7 \text{ V}$ and $I = 0.6 \text{ nA}$.

molecule is 0.68 nm, and the permanent dipole moment is close to 4.9 D (Figure 1a).

Figure 1b is a large-scale STM image acquired on the Si(111)-B $\sqrt{3x\sqrt{3}R30^\circ}$ surface at room temperature after the deposition of 4-aminobenzonitrile. A well-ordered adlayer of molecules can be clearly observed. The formation of a parallel nanowire network is revealed by the high-resolution STM images, with an average distance measured between two nanolines equal to $0.5 \pm 0.1 \text{ nm}$ (Figure 1b). The elemental building blocks of the nanolines are constituted by two spots. Each spot ($0.6 \pm 0.1 \text{ nm}$) is assigned to one molecule (0.68 nm). The length of a pair of protrusions is $1.7 \pm 0.1 \text{ nm}$, which corresponds to two molecules separated by $0.6 \pm 0.1 \text{ nm}$ (Figure 1c). A close examination of the large-scale STM image (Figure 1b) shows the presence of two types of nanolines. This is highlighted in Figure 2a.

In one case, the nanowire is straight (Figure 2a, S) whereas in the other case, it takes a saw-toothed shape (Figure 2a, S-T). In the case of straight nanolines, the elemental cell is formed by one pair of molecules. The strong permanent dipole moment of 4-aminobenzonitrile (4.9 D) induces large dipole-dipole interactions between molecules which can take the well-known antiferroelectric configuration, with the cyano groups pointing in one toward the other (Figure 2c) despite the electrostatic repulsion.¹⁰

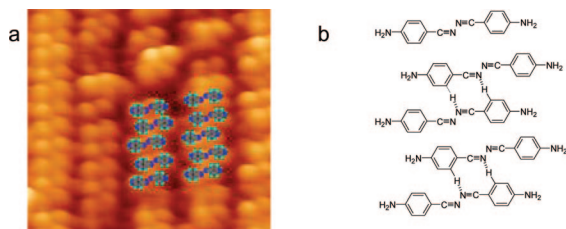


Figure 3. (a) Superposed ball model of 4-aminobenzonitrile on saw-toothed nanolines on STM image ($8 \times 10 \text{ nm}^2$, $V_s = -1.7 \text{ V}$ and $I = 0.6 \text{ nA}$); (b) hydrogen bonds between neighbor pairs of molecules.

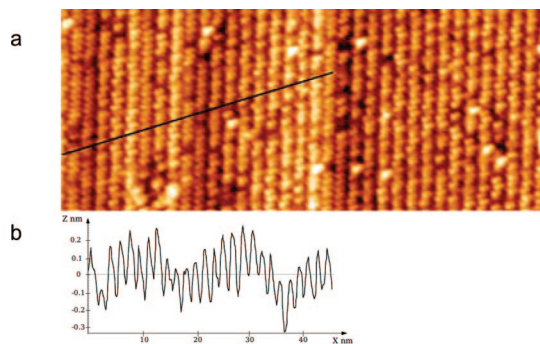


Figure 4. (a) Large scale STM image ($60 \times 25 \text{ nm}^2$, $V_s = -1.7 \text{ V}$ and $I = 0.6 \text{ nA}$) of the nanolines network on Si(111)-B $\sqrt{3} \times \sqrt{3} R30^\circ$ surface at room temperature and (b) z -profile along the dark line.

The size of the elemental (i.e. a pair of molecules) cell, about $0.8 \times 1.7 \text{ nm}^2$ measured by STM, is in agreement with the distances obtained with the model.

In the case of saw-toothed nanolines, the elemental cell takes a parallelogram shape with a size being about $1.7 \times 1.7 \text{ nm}^2$ and is constituted by two pairs of molecules (Figure 2a). Each pair preserves the antiferroelectric conformation of two molecules in order to keep the stability of the edifice. This reorganization can be explained by the formation of two hydrogen bonds between the nitrogen atom of the cyano group and the hydrogen atom on the 2-position of the aromatic ring (see Figure 3). These interactions are strongly supported by the electronic skeleton of 4-aminobenzonitrile.¹¹ Consequently, each pair of molecules can slip toward its neighbor to promote the interactions between the molecules and to align the three involved atoms, C–H \cdots N (Figure 3a). As all experiments were performed at room temperature, the diffusion of molecules on the substrate is possible and can lead to the reorganization of nanolines.

After this rearrangement, the nanolines are still preserved but they take a symmetric saw-toothed structure instead of a straight structure. This new conformation is more stable than the well-known antiferroelectric distribution because two hydrogen bonds per pair of molecules reinforce the interactions between the molecules in order to stabilize the complete adlayer. This hypothesis is justified by the presence, in the large scale STM images, of 12% of nanolines in the straight conformation and 88% in the symmetric saw-toothed conformation (see Figure 1b and 4a).

In a very large-scale STM image (Figure 4a), a modulation of the intensity appears as previously reported by K. Kern et al. in the case of deposition of (Z) 4-(2-pyrid-4-yl-vinyl)benzoic acid

on Ag(111).¹² According to these authors, the origin of this modulation is presumably explained by a vertical displacement of molecules to reduce strains. In our study, a vertical displacement of molecules is also visible (about 0.30 nm in Figure 4b). In accordance to Kern et al., the modulation of the intensity can be explained by the space limitations in molecular adlayer domains.

To sum up, for the first time, the formation of a complete adlayer of organic molecules has been achieved on semiconductive substrate at room temperature. This remarkable result is explained by the use of passivate Si(111)-B $\sqrt{3} \times \sqrt{3} R30^\circ$ surface and the formation of nanolines constituted by dipolar molecules. These molecules are paired to adopt the antiferroelectric arrangement. They optimize their dipole–dipole interactions and they are linked by two hydrogen bonds between two consecutive neighboring pairs of molecules. The high stability of the adlayer seems to be justified by the addition of these two types of interactions. This new method provides a versatile and easy approach to extend the supramolecular organization developed on metallic substrate to semiconductive substrates at room temperature.

Acknowledgment. The authors thank Dr. C. Joachim (CEMES, Toulouse, France) for fruitful discussions. This work is supported by the Communauté d'Agglomération du Pays de Montbéliard.

Supporting Information Available: STM experiments. This material is available free of charge via the Internet at <http://pubs.acs.org>.

References

- (1) Joachim, C.; Gimzewski, J. K.; Aviram, A. *Nature* **2000**, *408*, 541–508.
- (2) Stepanow, S.; Lingenfelder, M.; Dmitriev, A.; Spillmann, H.; Delvigne, E.; Lin, N.; Deng, X. B.; Cai, C. Z.; Barth, J. V.; Kern, K. *Nat. Mater.* **2004**, *3*, 229–231.
- (3) Lehn, J.-M. In *Supramolecular Chemistry: Concepts and Perspectives*, VCH:Weinheim, Germany, 1995.
- (4) (a) Barth, J. V.; Constantini, G.; Kern, K. *Nature* **2005**, *437*, 671–679. (b) Theobald, J. A.; Oxtoby, N. S.; Philipps, N. A.; Champness, N. R.; Beton, P. H. *Nature* **2003**, *424*, 1029–1031. (c) Percec, V.; Glodde, M.; Bera, T. K.; Miura, Y.; Shiyonovskaya, I.; Singer, K. D.; Balagurusamy, V. S. K.; Heiney, P. A.; Schnell, L.; Rapp, A. *Nature* **2002**, *419*, 384–387. (d) Grill, L.; Dyer, M.; Lafferentz, L.; Persson, M.; Peters, M. V.; Hecht, S. *Nat. Nanotechnol.* **2007**, *2*, 687–691.
- (5) (a) Li, S.-S.; Yan, H.-J.; Wan, L.-J.; Yang, H.-B.; Northop, B. H.; Stang, P. J. *J. Am. Chem. Soc.* **2007**, *129*, 9268–9269. (b) Puigmarti, J.; Minoia, A.; Uji-i, H.; Rovira, C.; Cornil, J.; De Feyter, S.; Lazzaroni, R.; Amabilino, D. B. *J. Am. Chem. Soc.* **2006**, *128*, 12602–12603. (c) Samori, P.; Yin, X.; Tchekborareva, N.; Wang, Z.; Pakula, T.; Jäckel, F.; Watson, M. D.; Venturini, A.; Müllen, K.; Rabe, J. P. *J. Am. Chem. Soc.* **2004**, *126*, 3567–3575. (d) Bléger, D.; Kreher, D.; Mathevet, F.; Attias, A.-J.; Schull, G.; Huard, A.; Douillard, L.; Fiorini-Debuisschert, C.; Charra, F. *Angew. Chem., Int. Ed.* **2007**, *46*, 7404–7407.
- (6) (a) Hamers, R. J.; Coulter, S. K.; Ellison, M. D.; Hovis, J. S.; Padowitz, D. F.; Scharz, M. P.; Greenlief, C. M.; Russel, J. N. *Acc. Chem. Res.* **2000**, *33*, 617–624. (b) Sloan, P. A.; Palmer, R. E. *Nature* **2005**, *434*, 367–371.
- (7) (a) Baffou, G.; Mayne, A. J.; Comtet, G.; Dujardin, G.; Sonnet, P.; Stauffer, L. *Appl. Phys. Lett.* **2007**, *91*, 073101. (b) Makoudi, Y.; Palmino, F.; Duverger, E.; Arab, M.; Chérioux, F.; Ramseyer, C.; Therrien, B.; Tschan, M. J.-L.; Süss-Fink, G. *Phys. Rev. Lett.* **2008**, *100*, 076405.
- (8) Harikumar, K. R.; Polanyi, J. C.; Sloan, P. A.; Ayissi, S.; Hofer, W. A. *J. Am. Chem. Soc.* **2006**, *128*, 16791–16797.
- (9) Makoudi, Y.; Arab, M.; Palmino, F.; Duverger, E.; Ramseyer, C.; Picaud, F.; Chérioux, F. *Angew. Chem., Int. Ed.* **2007**, *46*, 9287–9290.
- (10) Lacaze, E.; Alba, M.; Goldmann, M.; Michel, J.-P.; Rieutord, F. *Eur. Phys. J. B* **2004**, *39*, 261–272.
- (11) (a) Melandri, S.; Sanz, M. E.; Caminati, W.; Favero, P. G.; Kiziel, Z. *J. Am. Chem. Soc.* **1998**, *120*, 11504–11509. (b) Yokoyama, T.; Yokoyama, S.; Kamikado, T.; Okuno, Y.; Mashiko, S. *Nature* **2001**, *413*, 619–621.
- (12) Barth, J. V.; Weckesser, J.; Trimarchi, G.; Vladimirova, M.; De Vita, A.; Cai, C.; Brune, H.; Günter, P.; Kern, K. *J. Am. Chem. Soc.* **2002**, *124*, 7991–8000.

JA8001259